

AD-A166 577

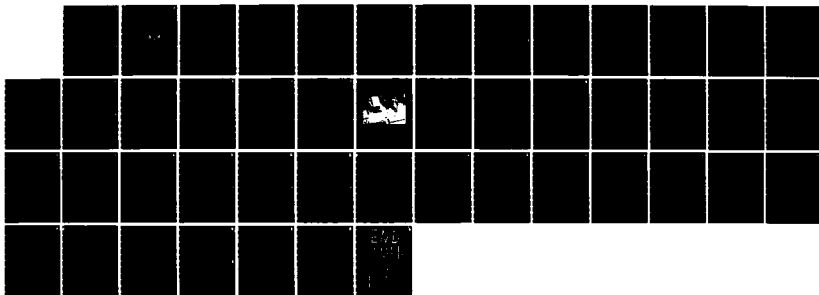
THE DEPENDANCE OF DAMAGE ACCUMULATION IN CARBON FIBRE
REINFORCED EPOXY CO. (U) ECOLE NATIONALE SUPERIEURE DES
MINES DE PARIS EVRY (FRANCE) C. A R BUNSELL ET AL.
DEC 85 AFOSR-84-0397

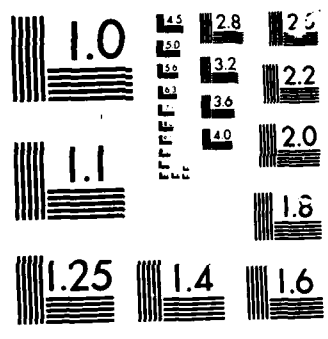
1/1

UNCLASSIFIED

F/G 13/13

NL





MICROCOPY

CHART

AD-A166 577

2

04

DTIC
S
APR 15 1986
J

DISTRIBUTION STATEMENT A
Approved for public release
Distribution Unlimited

OTIC FILE COPY

Contract U.S. AIR FORCE/ARMINES-
Centre des Matériaux

N° A.F.O.S.R. 84-0397
Final Report
December 1985

THE DEPENDANCE OF DAMAGE ACCUMULATION IN
CARBON FIBRE REINFORCED EPOXY COMPOSITES
ON MATRIX PROPERTIES

66 4 1 002

UNCLASSIFIED

ADA 166577

SECURITY CLASSIFICATION OF THIS PAGE

REPORT DOCUMENTATION PAGE

1a. REPORT SECURITY CLASSIFICATION UNCLASSIFIED			1b. RESTRICTIVE MARKINGS N/A	
2a. SECURITY CLASSIFICATION AUTHORITY UNCLASSIFIED			3. DISTRIBUTION / AVAILABILITY OF REPORT A	
2b. DECLASSIFICATION / DOWNGRADING SCHEDULE				
4. PERFORMING ORGANIZATION REPORT NUMBER(S)			5. MONITORING ORGANIZATION REPORT NUMBER(S) AFOSR-85-0397	
6a. NAME OF PERFORMING ORGANIZATION Ecole Nationale Supérieure des		6b. OFFICE SYMBOL (if applicable) N/A	7a. NAME OF MONITORING ORGANIZATION EOARD	
6c. ADDRESS (City, State, and ZIP Code) Mines de Paris, B.P. 87 F-91003 Evry Cedex France			7b. ADDRESS (City, State, and ZIP Code) Box 14 FPO NY 09510	
8a. NAME OF FUNDING / SPONSORING ORGANIZATION AFWAL		8b. OFFICE SYMBOL (if applicable) MLBM	9. PROCUREMENT INSTRUMENT IDENTIFICATION NUMBER	
8c. ADDRESS (City, State, and ZIP Code) Wright-Patterson AFB, OH 45433			10. SOURCE OF FUNDING NUMBERS	
			PROGRAM ELEMENT NO. 61102F	PROJECT NO. 2301
			TASK NO. D1	WORK UNIT ACCESSION NO. 185
11. TITLE (Include Security Classification) THE DEPENDANCE OF DAMAGE ACCUMULATION IN CARBON FIBRE REINFORCED EPOXY COMPOSITES ON MATRIX PROPERTIES (UNCLASSIFIED)				
12. PERSONAL AUTHOR(S) A.R. BUNSELL - B. PONSOT				
13a. TYPE OF REPORT FINAL SCIENTIFIC		13b. TIME COVERED FROM 30Sep84 TO 29Sep85	14. DATE OF REPORT (Year, Month, Day) DECEMBER 1985	15. PAGE COUNT 44
16. SUPPLEMENTARY NOTATION				
17. COSATI CODES			18. SUBJECT TERMS (Continue on reverse if necessary and identify by block number) Composites, Damage accumulation, Durability, Matrix properties	
FIELD	GROUP	SUB-GROUP		
19. ABSTRACT (Continue on reverse if necessary and identify by block number) Two types of fibre reinforced resin specimens have been tested, each having the same type of fibre but with very different resin systems. In this way the effect of matrix properties on carbon fibre reinforced resin systems has been studied. Steady loads on unidirectional specimens have confirmed that far from being the unresponsive purely elastic bodies that most measuring techniques suggest the acoustic emission technique reveals the continuous accumulation of internal damage. The acoustic emission behaviour is characterized by curves of $\ln(dt/dN)$ as a function of total accumulated emissions which typically shows two asymptotic slopes, one at the origin, the other at infinity. An analytical expression has been proposed to describe this behaviour involving four parameters. The rate of damage accumulation has been shown to be greatly influenced by the properties of the matrix, with an increased rate observed with a resin containing a high percentage of plasticizer. The histograms of the				
20. DISTRIBUTION / AVAILABILITY OF ABSTRACT <input checked="" type="checkbox"/> UNCLASSIFIED/UNLIMITED <input type="checkbox"/> SAME AS RPT <input type="checkbox"/> DTIC USERS			21. ABSTRACT SECURITY CLASSIFICATION UNCLASSIFIED	
22a. NAME OF RESPONSIBLE INDIVIDUAL			22b. TELEPHONE (Include Area Code)	22c. OFFICE SYMBOL

cont'd
amplitude distributions reveal a peak at 25 db at low stresses which is seen to be displaced towards 40 db at higher applied loads. It is concluded that the peak at 40 db is due to fibre failure whereas the lower peak may be due to microcracking of the matrix. The study has revealed that period of overloading are equivalent to accelerated mechanical aging at lower loads.



DEPARTMENT OF THE AIR FORCE
AIR FORCE OFFICE OF SCIENTIFIC RESEARCH (AFSC)
EUROPEAN OFFICE OF AEROSPACE RESEARCH AND DEVELOPMENT
BOX 14, FPO NEW YORK 09510

REPLY TO
ATTN OF: LTS/Autovon 235-4299

26 March 1986

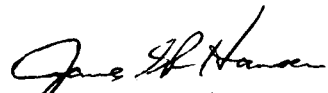
SUBJECT: EOARD-TR-86-04, Final Scientific Report, "The Dependence of Damage Accumulation in Carbon Fibre Reinforced Epoxy Composites on Matrix Properties

TO: DTIC/Air Force Liaison Representative
Cameron Station
Alexandria, VA 22304-6145

1. I certify that the subject TR has been reviewed and approved for public release by the controlling office and the information office in accordance with AFR 80-45/AFSC Sup 1. It may be made available or sold to the general public and foreign nationals.

2. Distribution statement A appears on the subject TR and the Form 1473 as required by AFRs 80-44 and 80-45.

FOR THE COMMANDER


JAMES G. R. HANSEN, Lt Col, USAF
Chief, Structures and
Structural Materials

2 Atchs

1. EOARD-TR-86-04 (2 cys)
2. DD Form 50

cc: EOARD/CMX
EOARD/CI

CONTRACT U.S. AIR FORCE/A.R.M.I.N.E.S. - Centre des Matériaux

N° A.F.O.S.R. 84-0397

Final Report

December 1985

THE DEPENDANCE OF DAMAGE ACCUMULATION IN CARBON
FIBRE REINFORCED EPOXY COMPOSITES ON MATRIX PROPERTIES

A.R. BUNSELL - B. PONSOT

S U M M A R Y

	<u>Pages</u>
I. INTRODUCTION.....	1
II. FAILURE MODEL.....	2
III. EXPERIMENTAL METHODS.....	12
III.1 Matrix systems.....	12
III.2 Composite fabrication.....	12
III.3 Specimens.....	14
III.4 Acoustic emission monitoring.....	14
IV. EXPERIMENTAL RESULTS.....	15
IV.1 Pure resin specimens.....	15
IV.2 Composite specimens.....	18
IV.3 Statistical analysis of the acoustic emission.....	29
V. CONCLUSION.....	33

Accession For	
NTIS CRA&I	<input checked="" type="checkbox"/>
DTIC TAB	<input type="checkbox"/>
Unannounced	<input type="checkbox"/>
Justification	
By	
Distribution /	
Availability Codes	
Dist	Avail and/or Special
A-1	



I. INTRODUCTION

The object of this study was to reveal the importance of the properties of the matrix in determining the rate of damage accumulation in carbon fibre reinforced epoxy resin. The specimens tested were in the form of flat plates which were subjected to mechanical loading. It is thought that a better understanding of the processes involved in damage accumulation will improve predictions of long term behaviour of composite structures.

In the case of unidirectional carbon-epoxy loaded parallel to the fibres it is known that the overall behaviour is elastic [1]. At the microscopic level however it has been shown that this is not the case and fibre failure under steady loads can be detected by the acoustic emission technique [2].

The role of the matrix in a composite is to ensure the structural integrity of the material. Reinforcement is assured by the fibres which can continue to contribute to the load bearing capacity of the composite, even if broken, due to load transfer by shearing of the matrix around the break which in this way is isolated. The length over which the matrix is sheared around a fibre break depends on the rigidity of the matrix and time dependent effects can be proposed if the matrix is viscoelastic.

In order to study the effects of matrix properties plate specimens were made with three types of resins having very different mechanical properties. These specimens were tested under various loading conditions and the internal damage which accumulated was monitored by acoustic emission and compared to a previously developed failure model [3].

II. FAILURE MODEL

No classical model based on fracture mechanics is able to predict failure in unidirectional carbon fibre epoxy specimens loaded parallel to the fibres. This is equally true for many filament wound structures in which the fibres are positioned to carry most of the applied stresses. Fracture mechanics assures that the material behaves as a continuum and fails by the propagation of two fracture surfaces. The composites considered in this study fails by the accumulation of internal damage which, in the absence of stress raisers, occurs throughout the body of the structure. Carbon fibre epoxy resin is usually considered as being perfectly elastic when loaded in the direction of the fibres however delayed failure of even unidirectional cfrp has been reported indicating non elastic behaviour and the time dependent accumulation of damage [4,5]. The viscoelastic properties of the matrix must be considered as being at the origin of this time dependent behaviour as it is known that carbon fibres are purely elastic at room temperature.

Rosen's model of failure of a unidirectional composite material is based on the weakest link idea and the failure scenario described below is based on a similar approach but taking into account the viscoelastic nature of the matrix [6]. The failure of a fibre in a bundle of fibres subjected to a steady load increases the load on all the other remaining intact fibres in the bundle. In the absence of a matrix the overload experienced by the intact fibre occurs at every point over their whole length. Subsequent failure of fibres will as a consequence be unrelated to the point of failure of the broken fibre and only due to the distribution of weakening defects on the fibres. If instead of a fibre bundle a unidirectional composite is considered the effect of the fibre break is restricted to a small section of the composite due to load transfer through the matrix at the broken ends of the fibre. The zone

over which the increase in load is experienced by fibres neighbouring a fibre break depends on the shear properties of the matrix, the quality of the interface and the Young's modulus of the fibre. If the properties of the matrix are time dependent this zone can increase in length along the fibre due to relaxation of the matrix and so its effect on neighbouring fibres will vary. This behaviour has been evoked by Rotem and Lifschitz to explain delayed failure in composites [7].

It has been observed that when unidirectional cfrp specimen is subjected to a constant load in the fibre direction the emission rate decreases with time. It is reasonable to assume that the emissions are directly related to internal damage accumulation and that in this case the principal source of emissions are fibre breaks. Laroche and Bunsell [2], studying a rigid matrix cfrp in which the resin was the CIBA GEIGY 914 C epoxy resin, showed that the rate of emissions obeyed a law of the form :

$$\frac{dN}{dt} = \frac{A}{t + \tau} \quad (1)$$

where t is time

τ a time constant

A a function of the applied stress .

Developing this relation we obtain :

$$\log \frac{dt}{dN} = \frac{N}{A} + \log \frac{\tau}{A} \quad (2)$$

so that the gradient of a plot of $\log \frac{dt}{dN}$ against $f(N)$ gives $\frac{1}{A}$.

A more general relationship was later proposed by Valentin and Bunsell [3] such that :

$$\frac{dN}{dt} = \frac{A}{(t + \tau)^n} \quad (3)$$

where n is a dimensionless parameter.

It was observed that for cfrp with a rigid matrix, $n = 0,99$ and the value of n represented the variation from linearity with the curve being more closely described by

$$\log \frac{dt}{dN} = \log \frac{\tau^n}{A} + \frac{n}{1-n} \log \left[1 + \frac{N (1-n)}{A \tau^{(1-n)}} \right] \quad (4)$$

Equation (4) has been successfully applied to the emission recorded from unidirectional plates subjected to steady loads. Long term tests reveal however that the curve tends to an asymptote. The curve therefore presents two asymptotes, one at the origin with a gradient $C1$ and at infinity of gradient $C2$. The asymptote at infinity is of particular importance as it is its stage which describes damage accumulation during long term steady loading and which can indicate time to failure. The acoustic emission behaviour tends to the second asymptote very quickly in the case of rigid matrices, loaded parallel to the fibres as described previously [2, 3]. The use of more flexible resins emphasizes the initial behaviour.

As a first approach it has been assumed that the acoustic emission behaviour results from two distinct mechanisms resulting in different emission rates but governed by the same type of law such that :

$$\frac{dN}{dt} = \frac{A_1}{t + \tau_1} + \frac{A_2}{t + \tau_2} \quad (5)$$

with $A_2 \gg A_1$ and $\tau_2 \gg \tau_1$

This expression was proposed by Valentin [8] in order to describe the acoustic emission behaviour of crossplied cfrp specimens with $(+45^\circ)_s$ and $(+30^\circ)_s$ lay ups. A second approach is to modify the initial expression by adding a term which become negligible as the number of emissions increases.

Thus, the initial expression proposed by Laroche and
Bunsell [2]

$$N = A \log \frac{t + \tau}{\tau}$$

becomes :

$$N = a \log \left(\frac{t + c}{b} \right) + g(N) \quad (6)$$

where a, b, c are constants

t the time

g(N) tends to zero as N tends to N_{\max}

N = 0 when t = 0

So that :

$$a \log \frac{c}{b} + g(0) = 0$$

and
$$C = b \exp \left(- \frac{g(0)}{a} \right)$$

If we write :

$$a = 1/K_1.$$

$$b = K_2.$$

$$C = K_2 \exp \left[- K_1 g(0) \right]$$

we have :

$$N = \frac{1}{K_1} \log \left(\frac{t + K_2 \exp (-K_1 g(0))}{K_2} \right) + g(N)$$

Putting :

$$N = 0 \text{ and } t = 0$$

we obtain :

$$\frac{t + K2. \exp [- K1. g(0)]}{K2} = \exp [K1 (N - g(N))]$$

so that :

$$t = K2 [\exp [K1 (N - g(N))] - \exp (- K1. g(0))] \quad (7)$$

and :

$$\frac{dt}{dN} = K1. K2 (1 - \frac{dg}{dN} (N)) \exp [K1 (N - g(N))]$$

therefore :

$$\log \frac{dt}{dN} = \log (K1 K2) + \log (1 - \frac{dg}{dN} (N)) + K1 (N - g(N)) \quad (8)$$

with $g(N) \rightarrow 0$

when $N \rightarrow N_{\max}$

If we put $\frac{dg}{dN} (N) \rightarrow 0$

when $N \rightarrow N_{\max}$

equation (8) gives a straight line for $\log \frac{dt}{dN}$ as a function of N when N becomes large.

We have therefore a general expression which includes two constants K_1 and K_2 and a function of N which has still to be defined. The experimental curve obtained by recording $\log \frac{dt}{dN}$ as a function of N can be described by four constants C_1, C_2, C_3, C_4 as shown in Figure 1 where :

C_1 is the gradient at the origin

C_2 is the gradient at infinity

C_3 is the ordinate of the second asymptote at $N = 0$

C_4 is the ordinate of the curve at $N = 0$

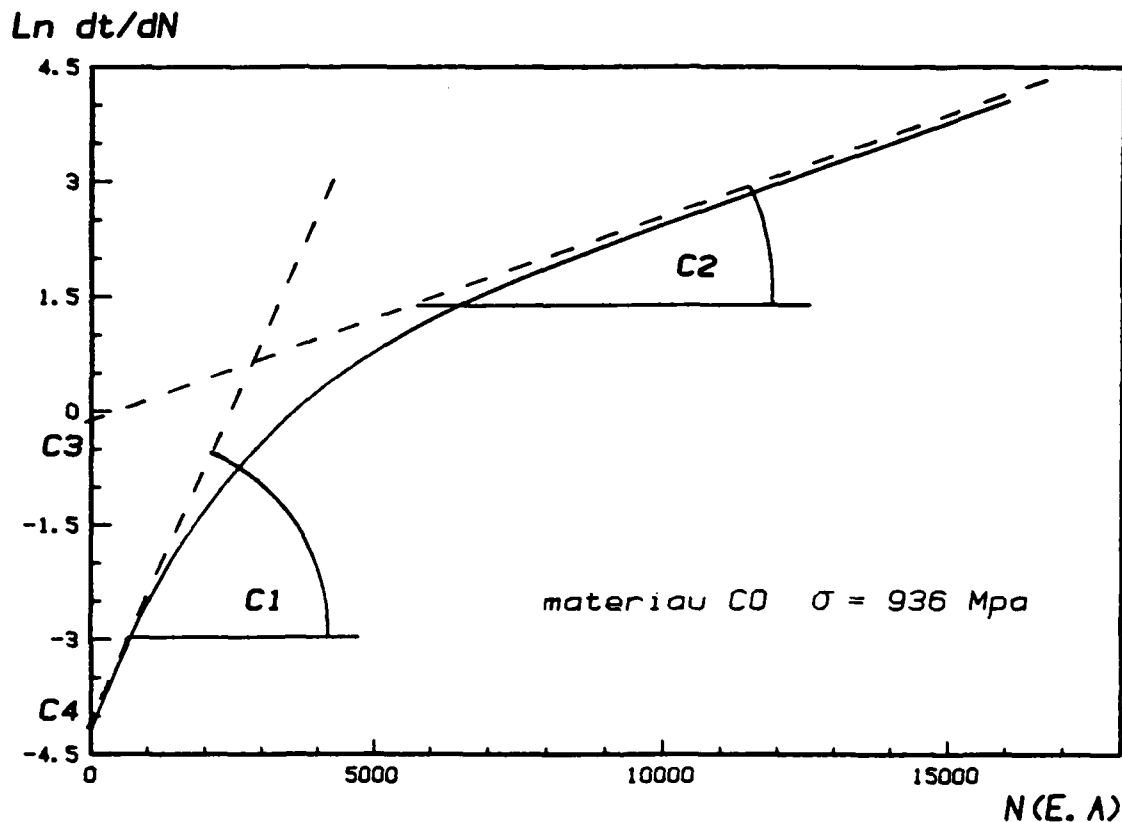


Figure 1 : Experimental curve giving the four constants C_1, C_2, C_3, C_4 .

It is therefore necessary to calculate the constants K_i as a function of the constants C_i .

The gradient of the curve at the origin C_1 is :

$$\frac{d \left(\log \frac{dt}{dN} \right)}{dN} = K_1 - K_1 \frac{dg}{dN} (N) + \frac{- \frac{dg^2}{dN^2} (N)}{1 - \frac{dg}{dN} (N)} \quad (9)$$

$$C_1 = \lim_{N \rightarrow 0} \frac{d \left(\log \frac{dt}{dN} \right)}{dN} (N)$$

$$N \rightarrow 0$$

The gradient at infinity C_2 :

$$C_2 = \lim_{N \rightarrow N_{\max}} \frac{d \left(\log \frac{dt}{dN} \right)}{dN} (N) \quad (10)$$

$$N \rightarrow N_{\max}$$

If we put $\frac{dg^2}{dN^2} (N) \rightarrow 0$ when $N \rightarrow N_{\max}$ we see that $C_2 = K_1$

as under these conditions $\frac{dg}{dN} (N)$ tends to 0

The ordinate of the asymptote at $N=0$ giving C_3 is described by an equation of the form :

$$H(N) = \log K_1 K_2 + K_1 \cdot N$$

$$\text{putting } N = 0 \quad H(0) = \log K_1 K_2$$

$$\text{so that } C_3 = \log K_1 K_2$$

$$(11)$$

The ordinate for the curve when $N = 0$ gives C_4 so that :

$$C_4 = \log K_1 K_2 + \log \left(1 - \frac{dg}{dN}(0)\right) - K_1 \cdot g(0) \quad (12)$$

The following conditions are therefore necessary as N tends to N_{\max}

$$g(N), \frac{dg}{dN}(N), \frac{d^2g}{dN^2}(N) \rightarrow 0$$

Putting $g(N)$ in the form $g(N) = \exp [-K_3 N + K_4]$

with $K_3 > 0$ we see from equation (8) that :

$$\log \frac{dt}{dN} = \log K_1 K_2 + \log (1 + K_3 e^{-K_3 N + K_4}) + K_1 (N - e^{-K_3 N + K_4}) \quad (13)$$

with the following conditions for the constants :

$$(a) \quad C_1 = K_1 (1 + K_3 e^{K_4}) - \frac{K_3^2 e^{K_4}}{1 + K_3 e^{K_4}}$$

$$(b) \quad C_2 = K_1$$

$$(c) \quad C_3 = \log K_1 K_2$$

$$(d) \quad C_4 = \log K_1 K_2 + \log (1 + K_3 e^{K_4}) - K_1 e^{K_4}$$

If

$$(e) \quad K5 = 1 + K3 e^{K4} \text{ with } K5 > 1 \text{ as } K3 > 0.$$

such that
$$e^{K4} = \frac{K5 - 1}{K3}$$

$$(a) \quad -K3 = (C1 - C2K5) \frac{K5}{K5 - 1}$$

$$(d) \quad C3 - C4 + \log K5 + \frac{C2 (K5 - 1)^2}{(C1 - C2 K5) K5} = 0$$

we have $C3 - C4 > 0 \quad C3 > C4$

$$\log K5 > 0 \quad K5 > 1$$

$$C2 > 0$$

which gives : $C1 - C2K5 < 0 \text{ ou } K5 > \frac{C1}{C2}$

As the gradient at the origin is always greater than the gradient at infinity we have $C1 > C2$ which verifies the relation :

$$K5 > \frac{C1}{C2} > 1.$$

We therefore have a non linear relationship for $K5$ (d) which can be solved by a numerical method so allowing $K3$ and $K4$ to be calculated

$$(a) \quad K3 = (C2K5 - C1) \frac{K5}{(K5 - 1)}$$

$$(e) \quad K4 = \log \left(\frac{K5 - 1}{K3} \right)$$

It is only necessary to adjust the values of the four constants K_1 , K_2 , K_3 , K_4 as a function of the experimental points as explaining in Annex 1. In this way an expression for the diagram of $\log \frac{dt}{dN}$ as a function of $f(N)$ is obtained

$$\log \frac{dt}{dN} = \log K_1 K_2 + \log (1 + K_3 e^{-K_3 N} + K_4) + K_1 (N - e^{-K_3 N + K_4}) \quad (13)$$

An example of this calculation is given in Figure 2 and it can be seen how the experimental values fit the calculated curve very closely.

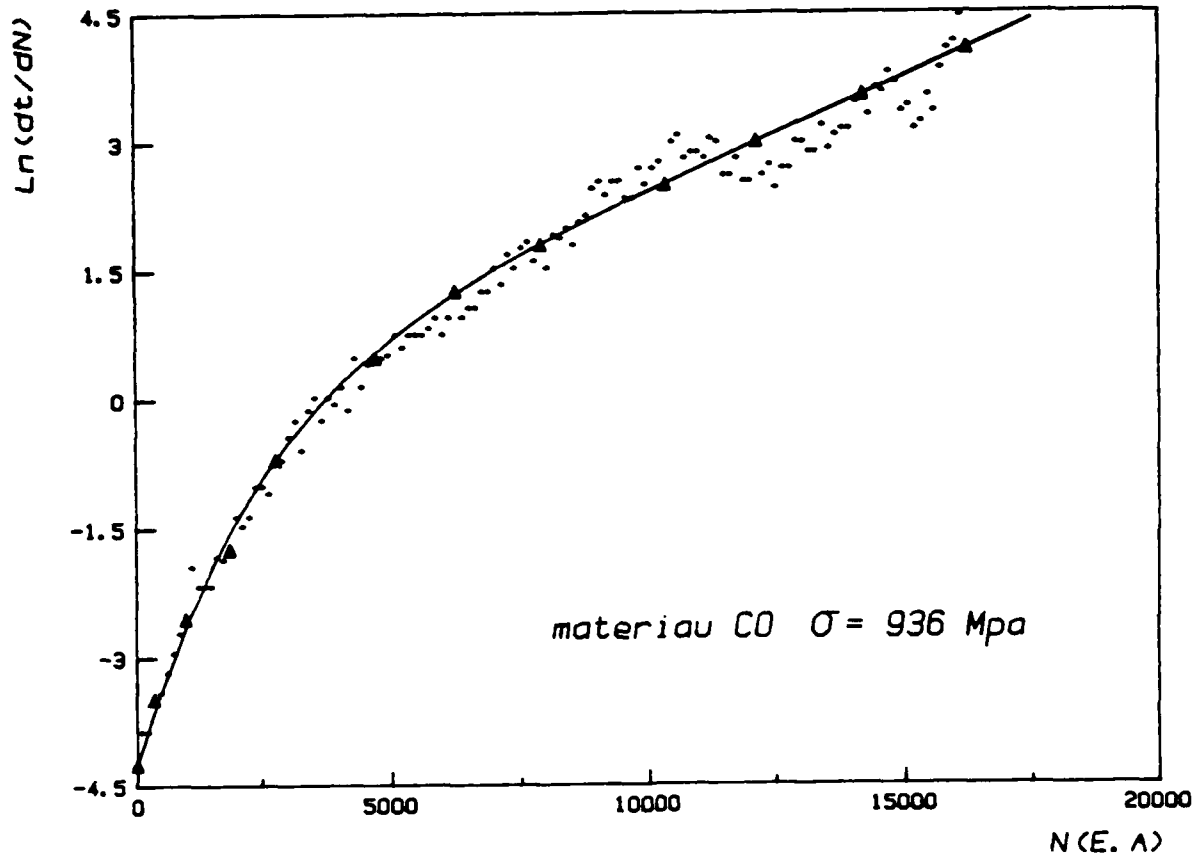


Figure 2 : Exemple of a calculated curve fitting experimental values

III. EXPERIMENTAL METHODS

III-1. Matrix systems

In order to test composites reinforced with the same type of carbon fibres (T300) but with matrix materials with very different behaviours it was necessary to make our own specimens from unimpregnated tow and different types of resins. The resin systems were chosen as they gave very different properties, particularly in elongation and creep behaviour but should not be considered as possible systems for composite structures.

Two such systems were made using different ratios of the CIBA GEIGY resins CY 208 a plasticizer and CY 205 as shown in Table (1). The two systems gave resins with very different properties.

	CY 208	CY 205	Fibres
Composite C0	70 %	30 %	T 300-B
Composite C1	30 %	70 %	T 300-B

Table (1) : Formulation of the resin systems studied

III-2. Composite fabrication

Unidirectional plates were made by filament-winding on a machine developed for this study and shown in Figure 3. The fibre tow passed into a heated bath containing the resin system and was impregnated by the resin. After leaving the bath, excess resin was removed from the tow as it passed over a free turning

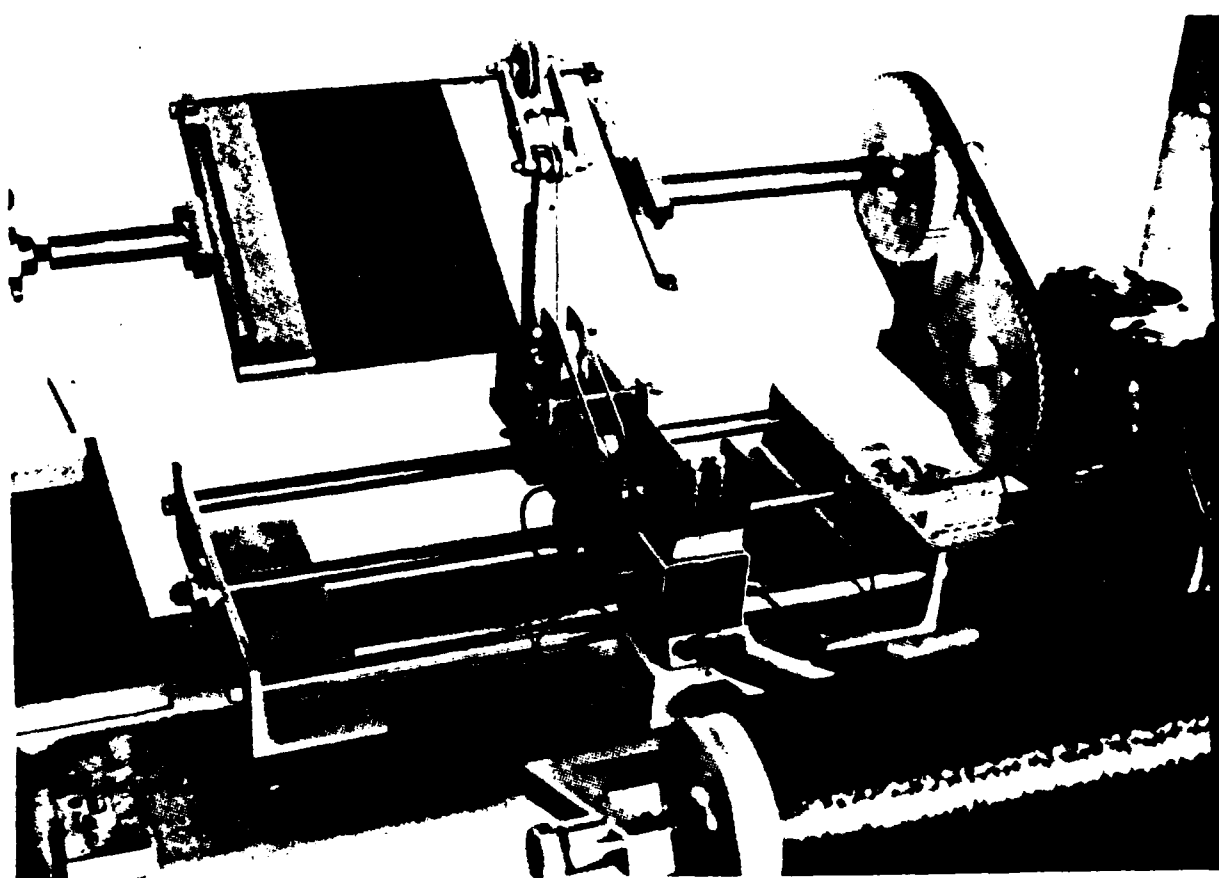


Figure 3 : Impregnation and filament winding apparatus

drum. The tow was then wound onto a mandrel in the form of a flat plate. Curing of the system took place after filament winding was complete and involved hot pressing the material using two flat plates which were placed against the mandrel.

III-3 . Specimens

Unidirectional specimens were cut from the plates which had been made as described above. The specimens were 17 mm Wide and 0.7 mm thick. Steel tabs were glued to each end of the specimens to protect them in the grips of the tensile machine. The tabs and specimens were drilled so that the load was transferred via a circular pin. The gauge length of the specimens was 100 mm. The fibre volume fraction was measured to be of around 53 %.

Pure resin specimens were cut from plates made with the proportions shown in table (1). These specimens were 15 mm wide by 4 mm thick with a gauge length of 30 mm. It was necessary to develop a strain measurement technique capable of measuring strain of 60-70 %. The gauges consisted of two induction displacement transducers giving a total displacement of 70 mm. To avoid problems of flexing the average of the two signals was used.

III-4 . Acoustic Emission Monitoring

All tests were monitored with a Dunegan-Endevco 3000 series acoustic emission apparatus. A piezo electric transducer, type D140B was used with a resonance frequency at about 200 KHz. The transducer was fixed to the centre of the specimen and acoustic coupling ensured by silicone grease.

Amplification of the signal was of 95 db (40 db from the preamplifier and 55 db from the main amplifier). The counting system used a threshold level of 25 db, the db measurements were given in reference to a signal of 1 μ V at the transducer. The signal was then analyzed as the number of accumula-

ted pulses, or by the use of an envelope generator as the number of events by introducing a dead time period after the recording of each signal. The dead time was chosen to be 100 μ s. In addition a logarithmic time base with a reset to zero after a fixed number of events ΔN was also used. In this way it was possible to plot directly the curve of $\ln dt/dN$ as a function of N .

IV. EXPERIMENTAL RESULTS

IV-1 . Pure resin specimens

The aim of these tests was to reveal the differences of behaviour between the two types of resins used. Table (2) gives the properties measured with each type of resin.

Resin	σ_R (MPa)	ϵ_R (%)	σ_Y (MPa)	ϵ_Y (%)	E (MPa)
R 0	40	4	13	0,6	2200
R 1	50	1	25	0,6	4000

Table (2) : Properties of the two resin systems employed

Tensile tests were conducted at a strain rate of 8 mm/mn. There was considerable scatter in the results of strength and failure strain, most probably due to internal defects produced during manufacture. It was decided to characterize the material as a function of the pseudo-yield stress σ_Y beyond which the behaviour was no longer linear, see Figure 4.

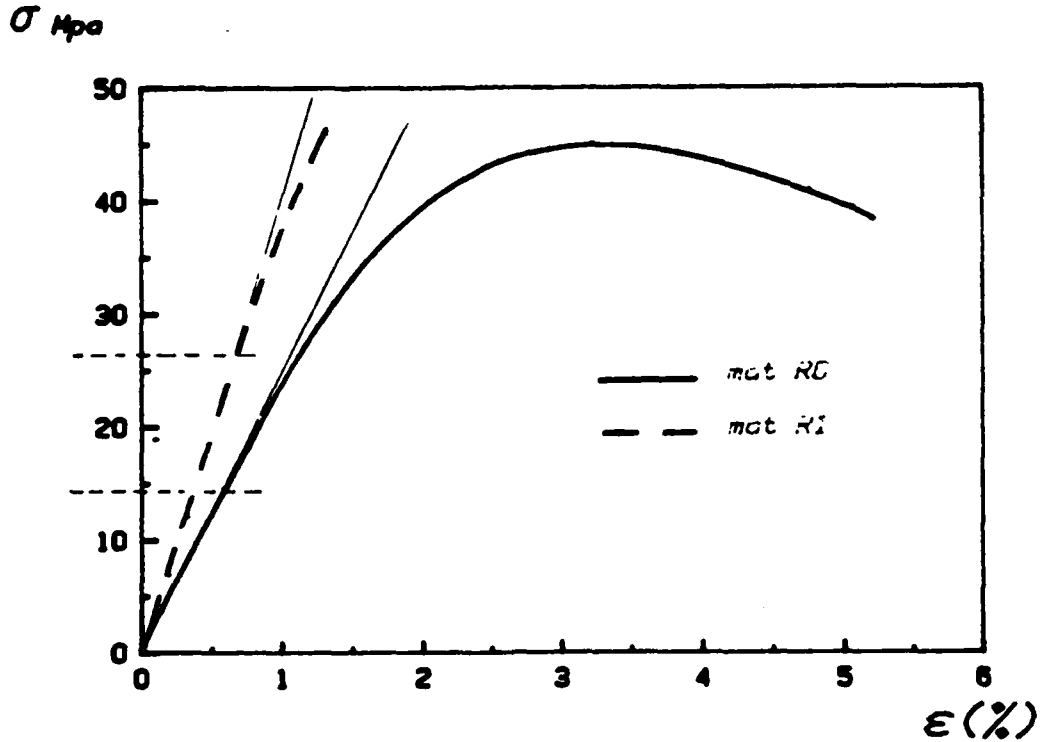


Figure 4 : Stress-strain curves of the two resin systems

Creep tests were conducted with reference to the pseudo yield stress and were conducted on a Mayes creep machine. The R0 resin deformed greatly with breaking strains often being of about 60 %. It was assumed as a first approximation that the volume of the specimen remained constant so that :

$$\sigma(t) = \sigma(0) \times [1 + \epsilon(t)]$$

In order to compare the behaviour of the two materials we could also study the evolution of the modulus $E(t)$ or its compliance

$$D(t) = 1/E(t)$$

$$\text{so that } E(t) = \frac{\sigma(t)}{\epsilon(t)} = \frac{\sigma(0) \cdot [1 + \epsilon(t)]}{\epsilon(t)}$$

$$D(t) = \frac{\epsilon(t)}{\sigma(0) \cdot [1 + \epsilon(t)]}$$

The results of several tests are shown in Figure 5. Two distinct regions can be seen which show clearly the differences in behaviour between the two resin systems. The composites made with the system R0 were therefore expected to reveal a greater effect of the time dependent properties of the matrix than the composites made with the R1 system. Lifschitz and Rotem [7] have shown that the stress along a broken fibre varies as a function of time such that:

$$\sigma(x,t) = \sigma_0 \cdot [1 - \exp\{-(J(t).A)^{-1/2}.x\}]$$

when $J(t)$ is the shear compliance
 t is the time
 x is the distance from the point of failure
 σ_0 is the stress in the fibre far from the failure

and $A = E_f \cdot r_f \cdot (r_m - r_f)/2$

where E_f is the fibre Young's modulus
 r_m is the radius of the cylinder of matrix around the fibre
 r_f is the radius of the fibre

We have studied the tensile compliance of these materials however it is to be noted that if $D_{R0}(t) > D_{R1}(t)$ then $J_{R0}(t) < J_{R1}(t)$ so that at the same distance x_1 from the failure and after the same interval of time t_1 we have :

$$\sigma_{C0}(x_1, t_1) < \sigma_{C1}(x_1, t_1)$$

It is therefore necessary to have a greater load transfer length with the resin system R0 and neighbouring fibres are therefore subjected to a higher load over a greater length than with the R1 system.

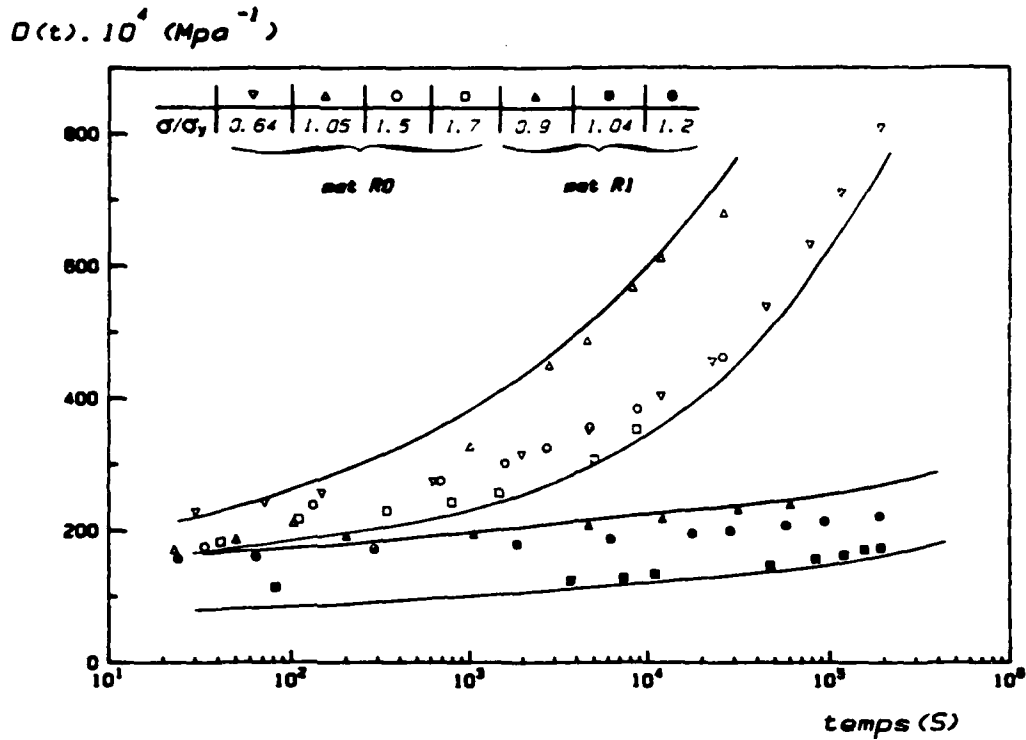


Figure 5 : Tensile compliance of the R0 and R1 resin systems

IV-2 . Composite specimens

- Tensile test :

In order to characterize the materials tensile tests were conducted on the two types of composites C0 and C1. Tests were conducted at a rate of 0,05 cm/mm. Table (3) gives the results

Composite	$\bar{\sigma}_R$ (MPa)	Mean deviation (MPa)
C0	1260	148
C1	1143	68

Table (3) : Mean results of tensile tests on the two composite systems

The average fibre volume fraction was 53 %. Figure 6 shows the acoustic emission recorded during a tensile test on the C0 material.

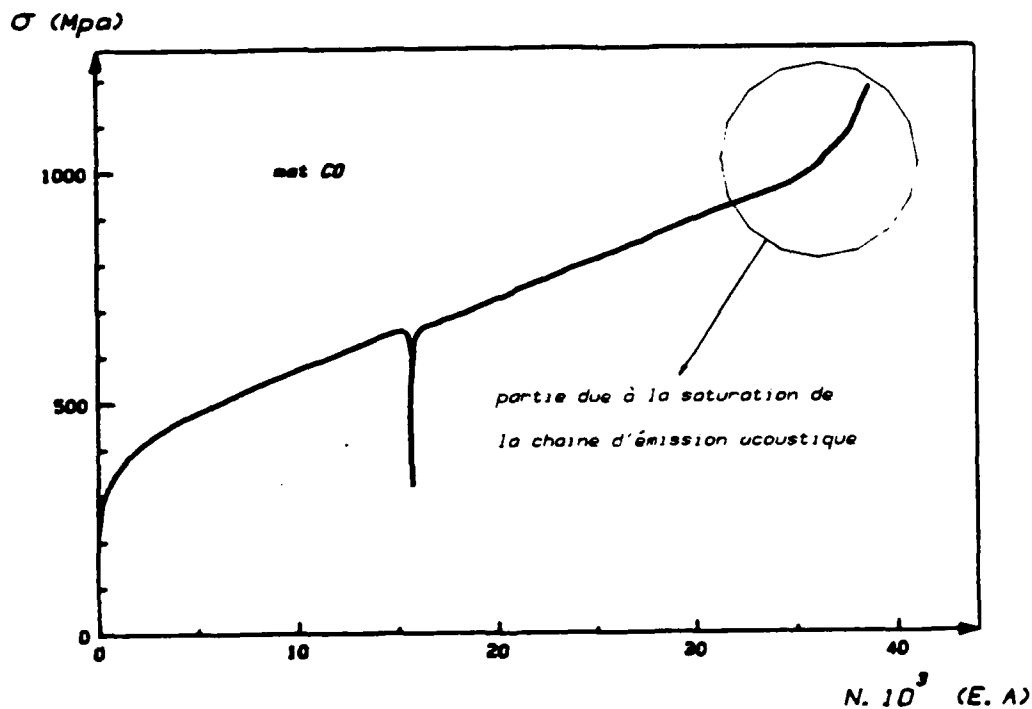


Figure 6 : Acoustic emission recorded during a tensile test on the composite C0

It was found that the Kaiser effect was more closely obeyed at the lower stress levels and that the more rigid composite material C1 showed closer adherence to the Kaiser effect than did the C0 material. Both materials began emitting at lower stresses than is reported for the more rigid T300-914 systems previously studied [8].

- Creep tests :

Creep tests at different load levels having stress ratios σ/σ_R from 0,4 to .1 were conducted. Below $\sigma = 0,4 \sigma_R$ negligible acoustic activity was recorded within reasonable time periods.

Table (4) gives typical results from a number of studies. The results for each specimen tested show the number of events recorded for each period of steady loading and the length of loading. In addition time necessary for composite C0 to accumulate the same number of events as recorded for the composite C1 was calculated from the equation

$$t = K2 [\exp(K1(N - \exp(-K3N + K4))) - \exp(-K1 \exp K4)]$$

where: t is in seconds

K1, K2, K3, K4 experimentally adjusted constants

N is the number of accumulated events at that load level

In all cases the time necessary to accumulate a given number of emissions was shorter for the C0 material than for the C1 material which reveals the greater speed of damage accumulation for the former composite. Figure 7 give examples of the stabilisation of the acoustic emission activity of the C0 unidirectional specimens.

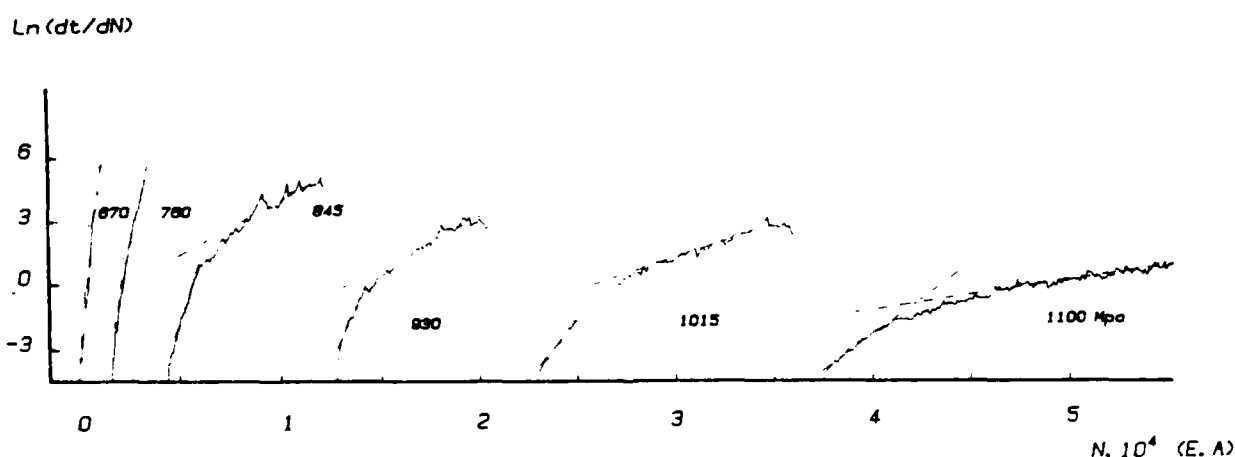


Figure 7 : Stabilisation of acoustic emission activity from unidirectional C0 specimens

It can be seen that damage accelerated at the higher

σ/σ_R	N(E.A.)	t(s)	N	t	N	t	N	t	N	t	N	t
0,41 - 0,45	-	-	2480 1040	$3.2 \cdot 10^5$ $8.45 \cdot 10^3$	1600	$3.84 \cdot 10^7$	1040	$2.23 \cdot 10^4$	-	-	-	-
0,46 - 0,50	1600 1760	$1.21 \cdot 10^4$ $1.878 \cdot 10^4$	-	-	-	-	-	-	1760	$1.15 \cdot 10^5$	-	-
0,51 - 0,55	4000 3120	$2.7 \cdot 10^3$ $9.2 \cdot 10^3$	7200 3120	$6.5 \cdot 10^5$ $6.5 \cdot 20^4$	2000 3120	$4.41 \cdot 10^5$ $9.1 \cdot 10^5$	-	-	3120	$2.89 \cdot 10^5$	-	-
0,56 - 0,60	13360 1360	$1.12 \cdot 10^5$ 127	9200 1360	$2.7 \cdot 10^5$ 312	9760 1360	$1.15 \cdot 10^6$ 526	1360	$3.32 \cdot 10^4$	-	-	-	-
0,61 - 0,65	24000 2720 2240 4320	$9.0 \cdot 10^4$ 739 448 $2.54 \cdot 10^3$	16960 2720 2240 4320	$2.6 \cdot 10^5$ 483 275 $2.07 \cdot 10^3$	15695 2720 2240 4320	$3.6 \cdot 10^5$ $1.68 \cdot 10^3$ 893 $7.92 \cdot 10^3$	2720	$6.18 \cdot 10^4$	2240	$5.06 \cdot 10^4$	4320	$1.99 \cdot 10^5$
0,66 - 0,70	-	-	18480 5200 6560	$5.38 \cdot 10^4$ 960 $1.899 \cdot 10^3$	20800 5200 6560	$1.83 \cdot 10^5$ $2.97 \cdot 10^3$ $6.71 \cdot 10^3$	-	-	5200	$3.54 \cdot 10^5$	6560	$7.33 \cdot 10^4$
0,71 - 0,75	20800 2800 12000	$4.99 \cdot 10^4$ 150 $8.18 \cdot 10^3$	-	-	30880 2800 12000	$7.43 \cdot 10^4$ 115 $5.34 \cdot 10^2$	2800	$3.87 \cdot 10^4$	-	-	12000	$2.14 \cdot 10^5$
0,76 - 0,80	-	-	-	-	-	-	8460	$5.46 \cdot 10^4$	5920	$9.33 \cdot 10^4$	-	-

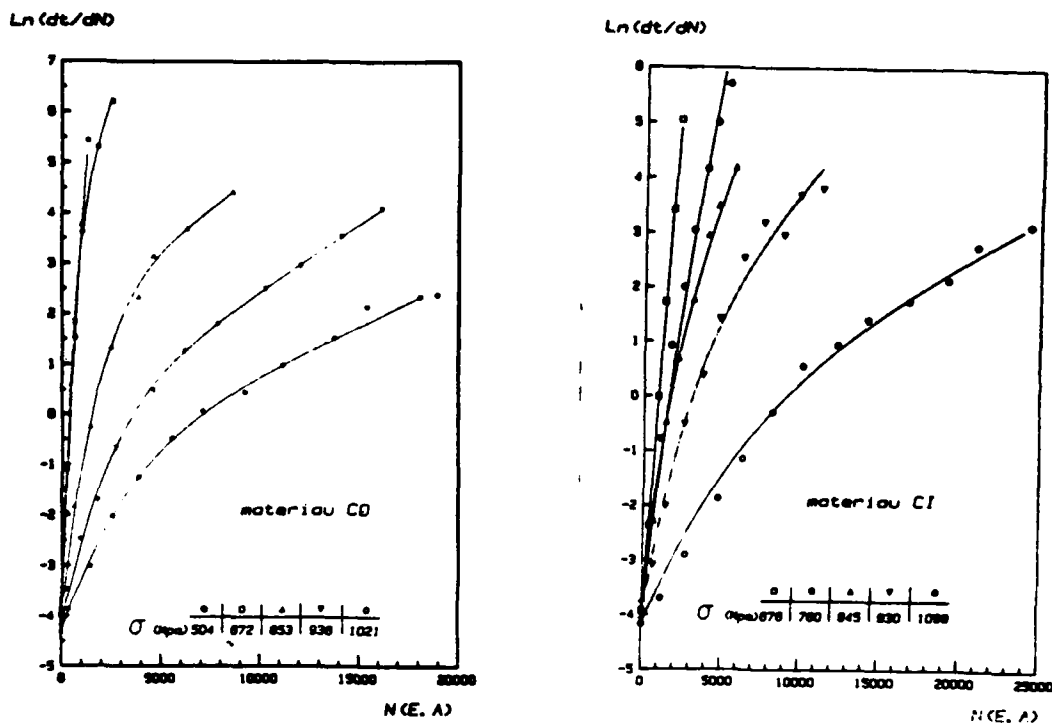
Mat 0

Mat 1

Table (4) : Results of creep tests on a number of plate specimens

loads. Figures 8 and 9 show similar curves for both the C0 and C1 specimens but all curves are drawn through the origin.

Figure 10 shows the evolution of the two composites at the same stress level. It can be seen that the C0 accumulates damage at all stress levels faster than the C1 specimens.



Figures 8 and 9 : Stabilisation of acoustic emission for the composite C0 and the composite C1

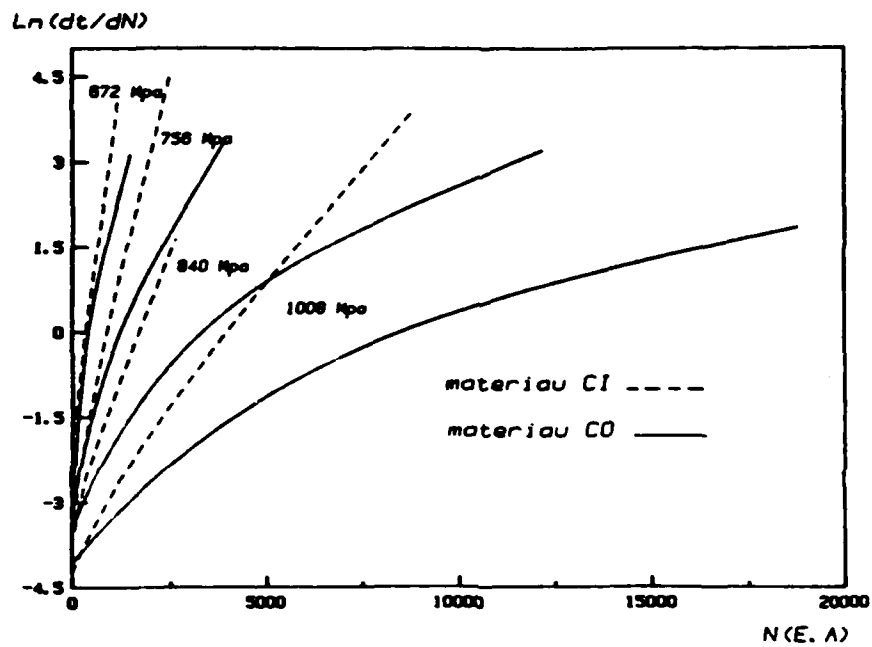


Figure 10 : Evolution of the composites C0 and C1 at the same stress level

It has not been possible to correlate the variation of the parameters K_I with physical processes. Figure 11 shows the variation of $\log K_I$ as a function of applied stress. The value of $\log K_I$ can be seen to decrease linearly as a function of increasing stress for both types of composite tested. The values of K_I for the C0 composites were always superior to those for the C1 composite, again revealing a more rapid accumulation of damage for the C0 specimens.

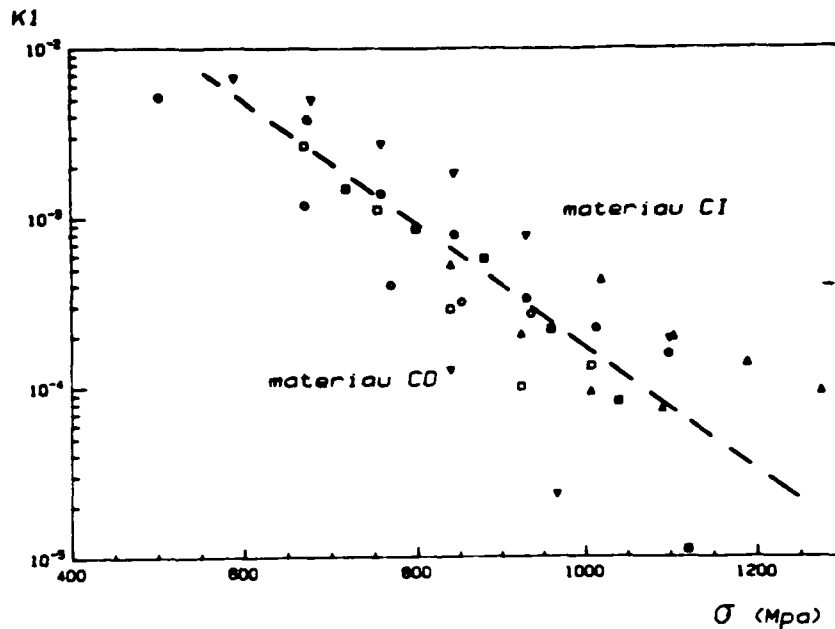


Figure 11 : Variation of K_I as a function of applied stress

- Loading sequence effects

Several specimens were held at different load levels and the loads increased or decreased during certain periods. An increase in load provoked an acceleration of emissions and produced a stabilisation giving a new value of K_I . It is significant to note that returning to the original load level produced acoustic activity which was practically that which would have been obtained by extrapolating the original curve as shown in Figure 12. In this way it can be seen that an increase in load was equivalent to a physical aging process as a much longer period would have been necessary at the lower load to accumulate the emissions recorded at the higher level.

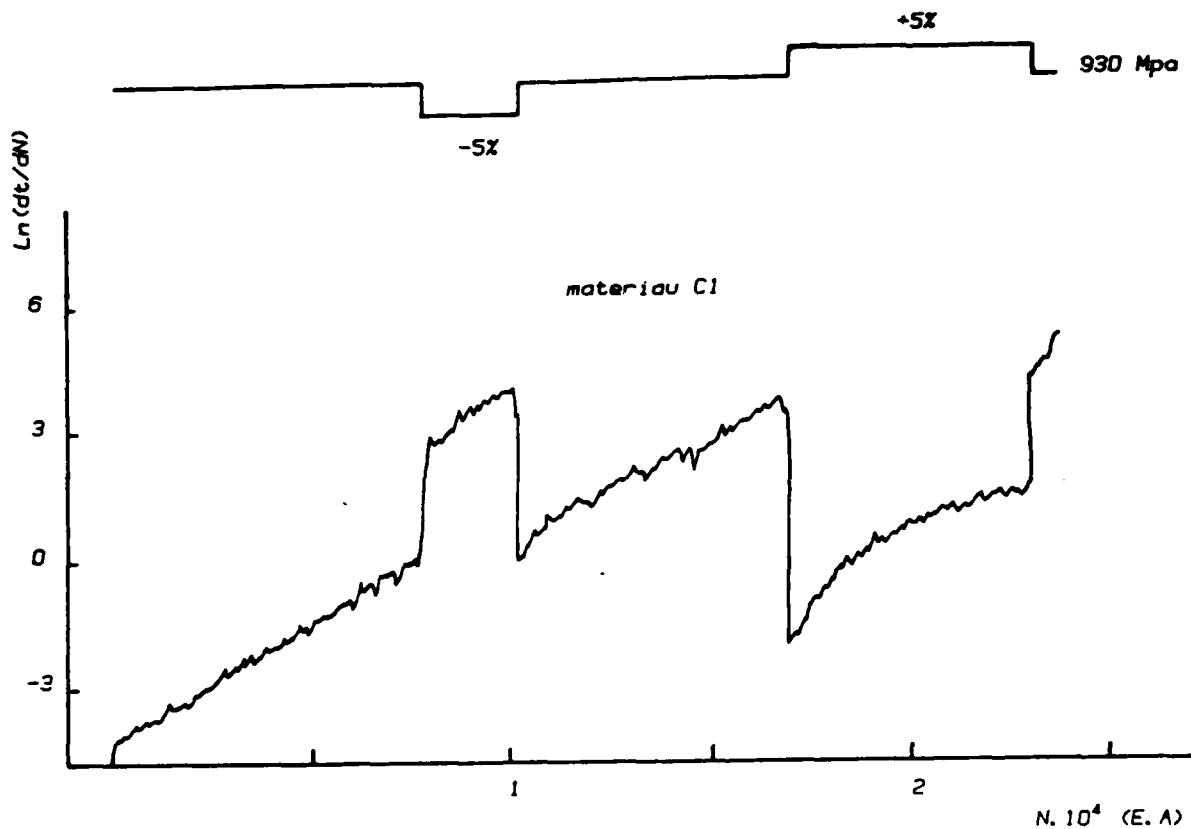


Figure 12 : Effect on acoustic emission rate of loading sequences

The acoustic emission rate was reduced by a reduction of load and a return to the original load level again produced the extrapolated behaviour.

- Effect of temperature

It has been shown that the viscoelastic properties of the matrix have a considerable effect on damage accumulation. The properties of the matrix can be affected by temperature and so studies were conducted on the composites at different temperatures. The temperature was modified during a period of steady loading on the composite C1. Figure 13 shows the results obtained .

An increase in temperature was found to produce an increase in emission rate. The stabilisation during the period of increased temperature was not regular probably due to the effect of internal stresses and thermal inertia . A return to the initial room temperature produces an extrapolation of the initial part of the curve. The effects of the change of temperature of the environment take sometimes to produce the change in the composite which explains a certain lag in acoustic emission behaviour. In this, an increase in temperature is analogous to the aging produced by an overload as explained earlier.

It proved possible to reproduce the results obtained with composite C0 at room temperature by testing the composite C1 at a raised temperature, once again emphasizing the importance of the viscoelastic properties of the matrix.

Tests on the composite C0 were also conducted at raised temperatures. The properties of the resin R0 were very temperature dependent and it was expected that as the temperature of the test was increased the load transfer length around fibre breaks would increase markedly . With an extremely soft matrix it could be expected that the behaviour of the fibre bundle would encountered. In this case emissions would cease altogether. This was found not to be the case however it was

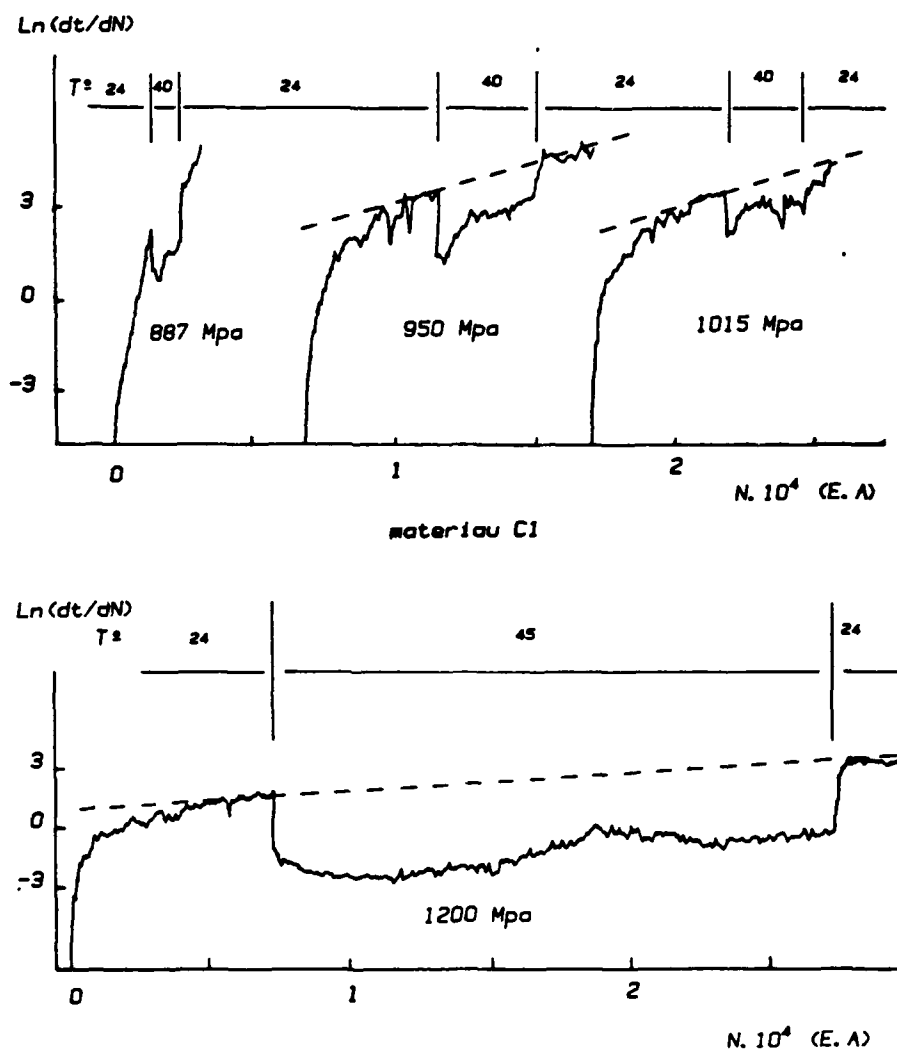


Figure 13 : Influence of temperature on the stabilisation of the acoustic emission during steady loading

observed that an increase in temperature of only a few degrees had a considerable effect on acoustic activity. Figure 14 shows that similar behaviour to that seen with composite C1 was obtained but for smaller increases in temperature. This observation has implications interpreting certain results obtained in a laboratory which was not temperature controlled. Figure 15 shows that acoustic activity of a C0 specimen showing two peaks at an interval of approximately twenty four hours.

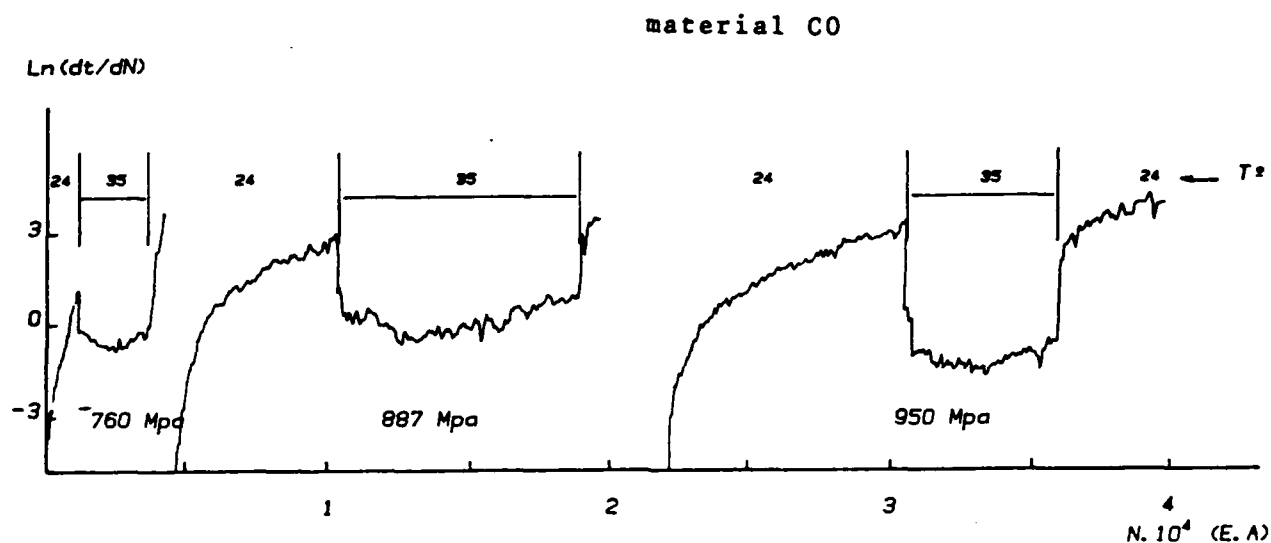


Figure 14 : Influence of a temperature change on acoustic emission during steady loading

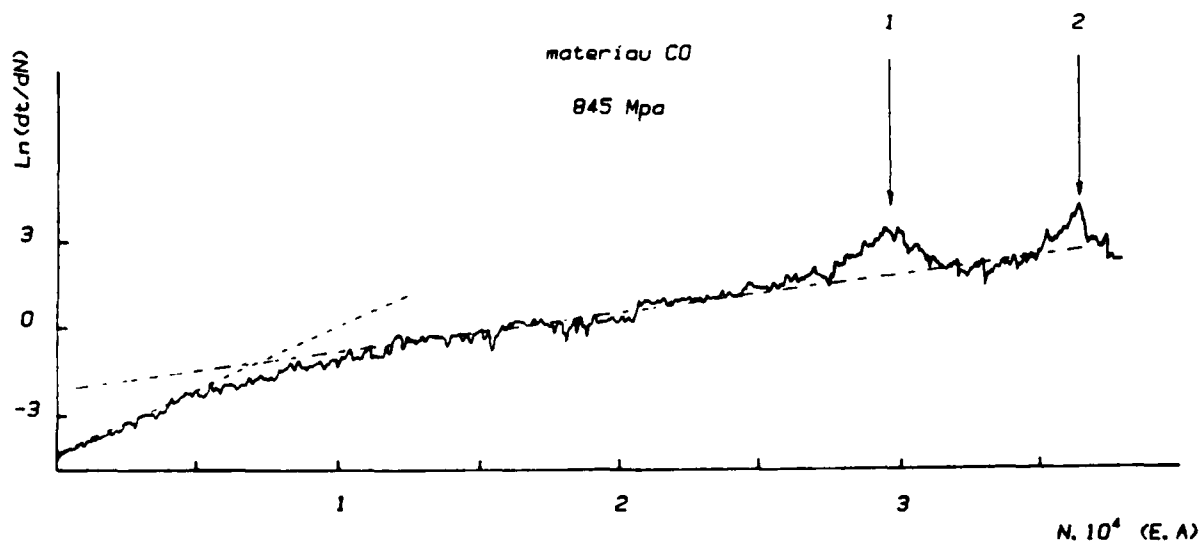


Figure 15 : Small changes in temperature in a laboratory between day and night were the most likely cause of the two peaks recorded

IV-3. Statistical Analysis of the Acoustic Emission

The acoustic activity monitored from a material can be characterized by several parameters

- number of emissions
- maximum amplitude
- duration
- energy

The acoustic emission chain used in this study allowed the first three types of analysis to be carried out. The response of the transducer to a pressure wave is schematically a damped sine wave with the form [9 , 10]

$$V = V_0 \exp(-\eta t) \sin \omega t$$

where η is the damping factor of the transducer

$$\omega = 2\pi U$$

V_0 = maximum amplitude

t = time

Certain parameters are interrelated, so that the energy depends on the square of the amplitude and the logarithm of the amplitude can be related to the number of emissions [10]. This being, we selected the signal amplitude as the characteristic parameter. The module used to record signal amplitude was the Dunegan-Endevco 921 module fitted to the 3 000 series apparatus immediately after the preamplifier. A threshold level of 25 db was chosen for all studies. The amplitudes were stored in the 921 amplitude analyser which had 101 memory stores classified from 0 to 100 db. The capacity of these memory stores was 4 096 events. The analog output giving signals from 0 to 10 volts allowed the distribution function to be traced directly on a recorder. In order to identify the evolution of amplitude histograms as a function of load, tensile tests on the unidirectional specimens were conducted and the load held steady at different levels. The amplitude histograms were recorded during each period of steady loading.

It was found that for a given hold time the number of

events recorded varied greatly between the first load level and the last. For these reasons, it was necessary to normalize the result at each load level by dividing the number of emissions of each amplitude level by the total number of emissions recorded during the hold period. Figures 16 and 17 show the results obtained at three load levels. In both cases it can be observed that the peak observed at 25 db at low stress levels increased to 40 db at higher stresses.

Several hypotheses can be advanced to explain this observation. The peak could be due to one type of mechanism which in the case of fibre failure liberates more energy at higher stress levels than at lower levels [11]. If two mechanisms are involved, one could dominate at higher stress levels. This would be the case if microcracking was at the origin of the 25 db peak and fibre failure the source of the 40 db peak. This second hypothesis although simplistic seems the most plausible as the shape of the histogram changes with the increasing load. There is little in the literature to which we can turn to help interpret these results although Shippen and Adams [12] attribute high amplitude peaks to fibre failure and low amplitude peaks to microcracking of the matrix. Finally it should not be forgotten that all of the fibres must be broken at least once in order to break the specimen and fibre failure must predominate near the final failure stage.

N/Nt

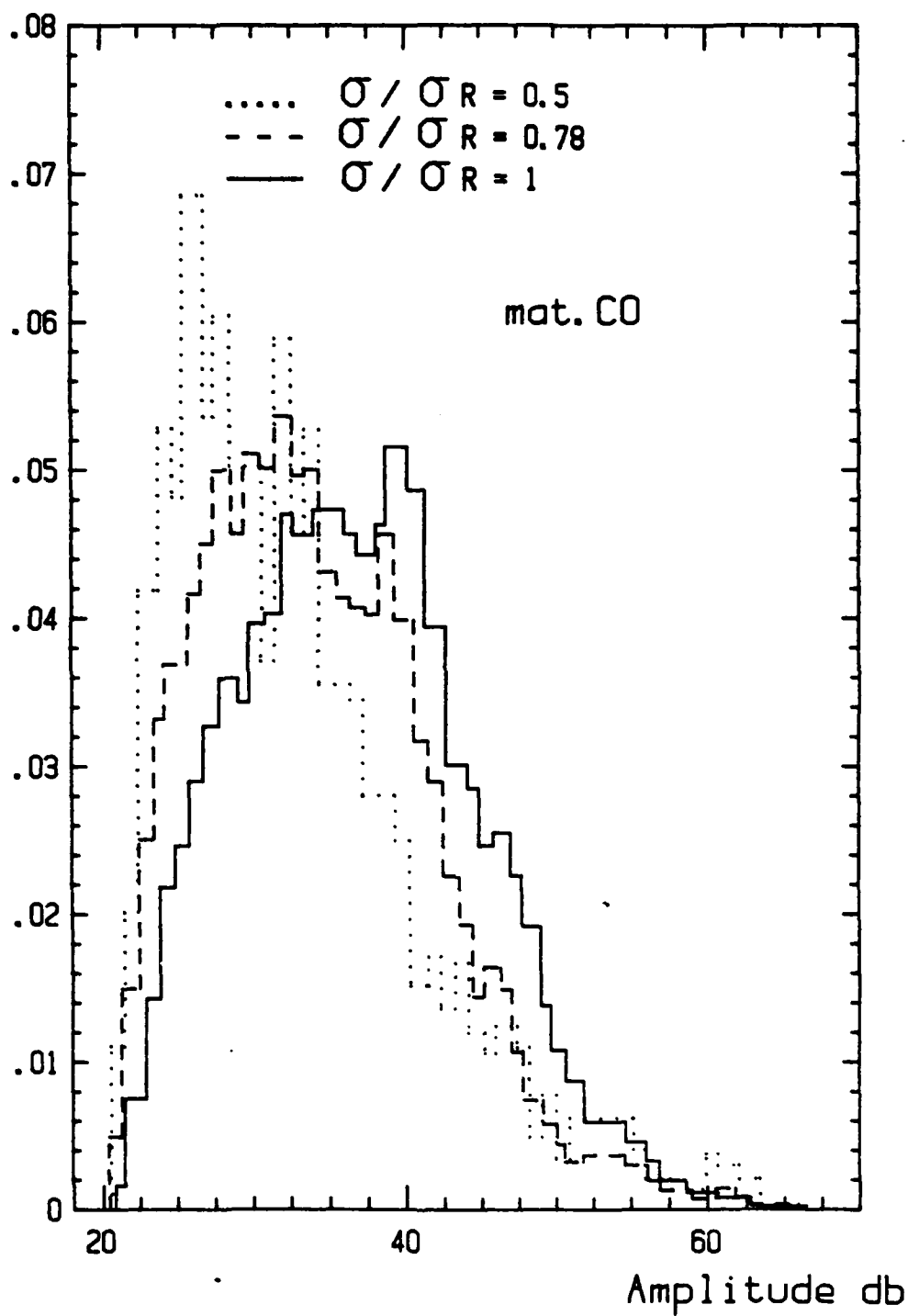


Figure 16 : Histograms of the amplitude distribution obtained with the CO specimen

N/Nt

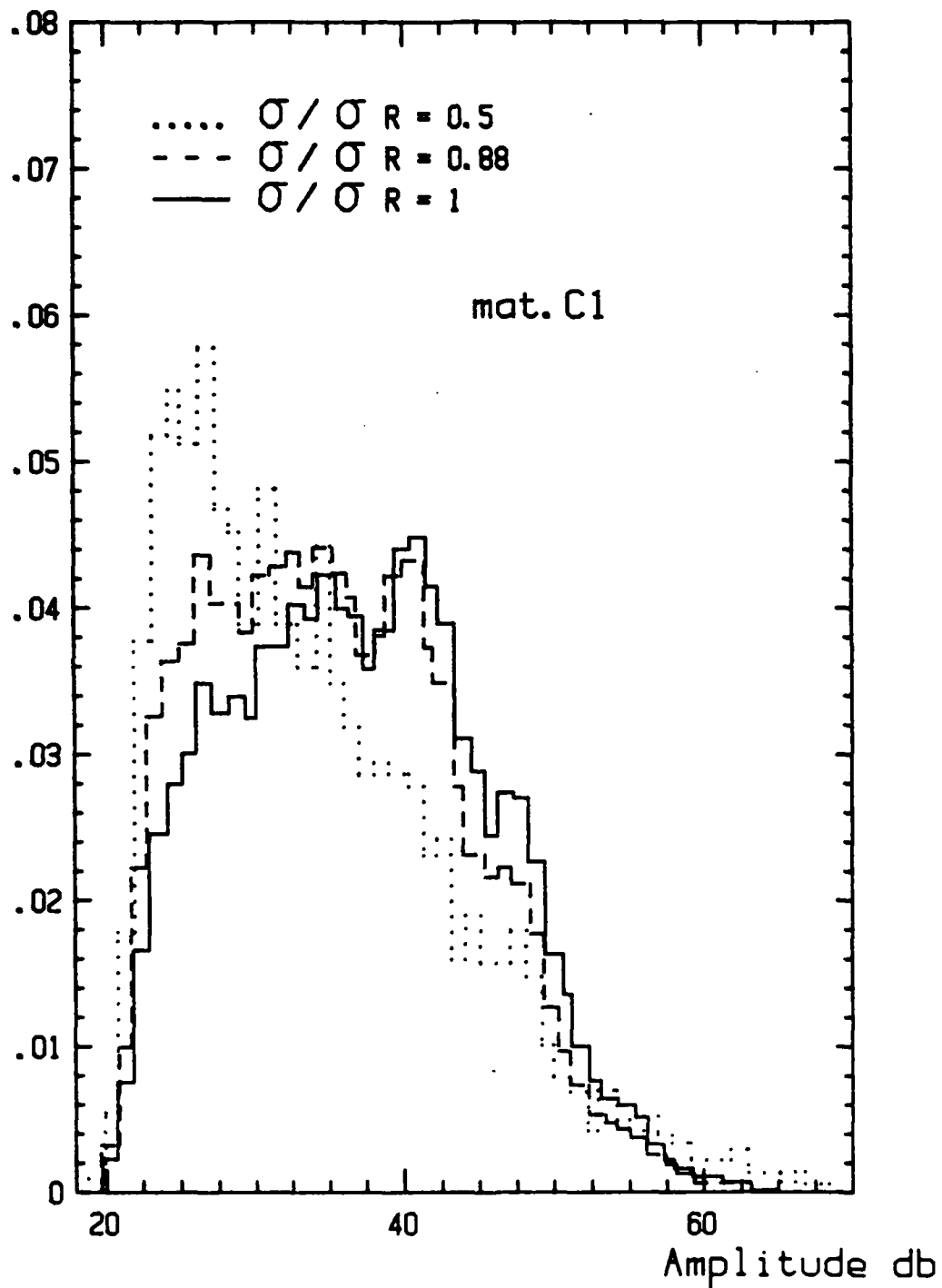


Figure 17 : Histograms of the amplitude distribution obtained with the C1 specimen

V. CONCLUSION

Two types of fibre reinforced resin specimens have been tested, each having the same type of fibre but with very different resin systems. In this way the effect of matrix properties on carbon fibre reinforced resin systems has been studied.

Steady loads on unidirectional specimens have confirmed that far from being the unresponsive purely elastic bodies that most measuring techniques suggest the acoustic emission technique reveals the continuous accumulation of internal damage. The acoustic emission behaviour is characterized by curves of $\ln(dt/dN)$ as a function of total accumulated emissions which typically shows two asymptotic slopes, one at the origin, the other at infinity.

An analytical expression has been proposed to describe this behaviour involving four parameters.

The rate of damage accumulation has been shown to be greatly influenced by the properties of the matrix, with an increased rate observed with a resin containing a high percentage of plasticizer.

The histograms of the amplitude distributions reveal a peak at 25 db at low stresses which is seen to be displaced towards 40 db at higher applied loads. It is concluded that the peak at 40 db is due to fibre failure whereas the lower peak may be due to microcracking of the matrix.

The study has revealed that period of overloading are equivalent to accelerated mechanical aging at lower loads. This is also true of temperature rises during steady loading which induces a more rapid rate of damage. This effect of accelerated aging could be turned to use in determining the long term behaviour of structures under load.

The acoustic emission technique is an indirect method of obtaining information concerning the damage of composite.

The signals arriving at the transducer do so from all over the material and are most probably considerably modified. Despite these difficulties the approach developed in this study offers a quantitative method of analysis of damage accumulation in carbon fibre reinforced resin composites.

REFERENCES

- [1] J.B. STURGEON, R.I. BUTT and L.W. LARKE
Creep of carbon fibre reinforced plastics.
R.A.E Technical report n° 76168 (1976)

- [2] D. VALENTIN, A.R. BUNSELL.
Stress and time dependent damage in carbon fibre
reinforced plastics.
Advances in Composites Materials, vol 11, (1980),
pp. 985-1000.

- [3] D. VALENTIN, A.R. BUNSELL.
A study of damage accumulation in carbon fibre
reinforced epoxy resin structures during mechanical
loading monitored by acoustic emission.
Journal of Reinforced Plastics and Composites,
(1982), pp. 314-334.

- [4] M. FUWA, A.R. BUNSELL and B. HARRIS.
Acoustic emission during cyclic loading of carbon
fiber reinforced plastics.
J. of Phys. D. appl. Phys. vol 8, (1975), pp. 1460.

- [5] M. FUWA, A.R. BUNSELL and B. HARRIS.
Tensile failure mechanisms in C.F.R.P.
J. of Materials Science, vol 10, (1975), pp. 2062-2070

- [6] B.W. ROSEN.
Tensile failure of fibrous composite.
A.I.A.A Journals, vol 2, (1964), pp. 1968-1991.

- [7] J.M. LIPSCHITZ, A. ROTEM.
Time dependent longitudinal strength of unidirectional
fibrous composites.
Fiber Science and Technology, vol 3, (1970), pp. 1-20.
- [8] D. VALENTIN, A.R. BUNSELL.
Contrôle par emission acoustique de l'endommagement
des composites à fibres de carbone.
Rapport final - Convention DRET/ARMINES n°79/503.
- [9] A. ROTEM.
The discrimination of microfracture mode of fibrous
composite material by acoustic emission technique.
Fiber Science and Technology, vol 10, (1977),
pp. 101-121.
- [10] D.O. HARRIS, R.L. BELL.
The measurement and signifiante of energy in acoustic
emission testing.
Experimental Mechanics, 17:347. [D-711].
- [11] P.W. BEAUMONT, B. HARRIS.
The energy of crack propagation in carbon fiber
reinforced resin systems.
J. of Mat. Science, vol 7, (1972), pp. 1265-1279.
- [12] N.C. SHIPPEN, D.F. ADAMS.
Acoustic emission monitoring of damage progression
in Graphite/Epoxy laminates.
J. of Reinforced Plastics and Composites, vol 7,
(1985), pp. 242-261.

A N N E X

1157

```

1  E = 1E4:EA = 1E4
2  A = 0
3  C$ = CHR$(4)
4  C = 0
5  U = 0:DI = 5:ZO = 0
6  PRINT
7  DI = 5:VI = 25
8  PRINT
9  INPUT "C1=":C1: INPUT "C2=":C2: INPUT "C3=":C3: INPUT "C4=":C4
10 PRINT D$:"PR#1": PRINT "VALEURS INITIALES"
11 PRINT "C1=":C1:" C2=":C2: PRINT : PRINT "C3=":C3:" C4=":C4: PRINT
12 PRINT D$:"PR#0"
13 DEF FN R(X) = C3 + LOG(X) + ((C2 * X + 2 - 2 * C2 * X + C2) / (- C2 * X
+ 2 + C1 * X)) - C4
14 DEF FN F(X) = LOG(K1 * K2) + LOG(1 + K3 * EXP(- K3 * X + K4)) + K1 *
(X - EXP(- K3 * X + K4))
15 DIM D(3): PRINT "VOULEZ-VOUS CHANGER LES PARAMETRES DE RECHERCHE (ACTUELS: +
OU - 5% ET 25 PAS)": INPUT A$
16 IF A$ = "N" THEN GOTO 25
17 PRINT "ENTREZ L'INTERVALLE DE RECHERCHE:": INPUT DI: PRINT "LE NOMBRE DE PAS
:": INPUT VI
18 GOTO 600
19 GOTO 3700
20 A = C1 / C2 + C1 / C2 * 1E - 3:B = C1 / C2 + 100
21 A1 = SGN(FN R(A))
22 B1 = SGN(FN R(B))
23 IF A1 * B1 = 0 THEN 360
24 IF A1 * B1 < 0 THEN 280
25 FOR I = 1 TO 1000
26 X = A + RND(2) * (B - A)
27 X1 = SGN(FN R(X))
28 IF X1 = 0 THEN 400
29 IF A1 * X1 < 0 THEN 270
30 NEXT I
31 B = X
32 D(2 + A1) = A
33 D(2 - A1) = B
34 Y = (D(1) + D(3)) / 2
35 Y1 = SGN(FN R(Y))
36 IF Y1 = 0 THEN 400
37 D(2 + Y1) = Y
38 IF ABS(D(1) - D(3)) / ABS(D(1) + ABS(D(3))) < 5E - 5 THEN 420
39 GOTO 320
40 IF A1 = 0 THEN 390
41 Y = B1
42 GOTO 430
43 Y = A1
44 IF ZO = 1 THEN GOTO 430
45 A = Y - (Y * 5 / 100):B = Y + (Y * 5 / 100):ZO = 1
46 GOTO 150
47 IF ZO = 1 THEN GOTO 440
48 A = Y - (Y * 5 / 100):B = Y + (Y * 5 / 100):ZO = 1
49 GOTO 150
50 XT = (C2 * Y - C1) * (Y / (Y - 1))
51 XD = (EXP(C3)) / C2
52 XL = LOG(Y - 1) / XD

```

```

450 GOTO 4000
460 RETURN
470 PRINT "VOULEZ-VOUS ?"
480 PRINT ""
490 PRINT "ENTRER LES POINTS EXPERIMENTAL.          AU CLAVIER:1"
500 PRINT ""
510 PRINT "ENTRER LES POINTS EXPERIMENTAUX          A PARTIR D'UN TABLEAU:2"
520 INPUT EN
530 IF EN = 1 THEN GOTO 1000.
540 INPUT "ENTRER LE NOMBRE DE POINTS EXPERIMENTAUX EX=":EX
550 DIM L(EX): DIM M(EX)
560 FOR I = 1 TO EX
570 M$ = "M(" + STR$(I) + ")=": PRINT M$
580 INPUT M(I)
590 L$ = "L(" + STR$(I) + ")=": PRINT L$
600 INPUT L(I)
610 NEXT I
620 PRINT ""
630 FOR I = 1 TO EX
640 PRINT "M(" + STR$(I) + ")=":M(I):" L(" + STR$(I) + ")=":L(I)
650 NEXT I
660 PRINT ""
670 PRINT "VALEURS A MODIFIER?(O/N)": INPUT VA$
680 IF VA$ = "N" THEN GOTO 840
690 PRINT "ENTRER LES VALEURS TAPER CONT PUIS RETURN EX:M(3)=2:L(3)=4:CONT"
700 STOP : GOTO 760
710 PRINT ""
720 INPUT "NOM DU TABLEAU (EXP):":T$
730 PRINT D$"OPEN":T$
740 PRINT D$"WRITE":T$
750 PRINT EX
760 FOR J = 1 TO EX
770 PRINT M(J)
780 PRINT L(J)
790 NEXT J
800 PRINT D$"CLOSE":T$
810 GOTO 1260
820 PRINT "NOM DU TABLEAU ?"
830 INPUT T$
840 PRINT D$"OPEN":T$
850 PRINT D$"READ":T$
860 INPUT EX
870 DIM M(EX): DIM L(EX)
880 FOR I = 1 TO EX
890 INPUT M(I): INPUT L(I)
900 NEXT I
910 PRINT D$"CLOSE":T$
920 FOR I = 1 TO EX
930 PRINT "M(" + STR$(I) + ")=":M(I):" L(" + STR$(I) + ")=":L(I)
940 NEXT I
950 PRINT "VALEURS A MODIFIER?(O/N)": INPUT VA$
960 IF VA$ = "N" THEN GOTO 1160
970 PRINT "ENTRER LES VALEURS TAPER CONT PUIS RETURN"
980 STOP : GOTO 1090
990 PRINT "VOULEZ-VOUS STOCKER LE TABLEAU?(O/N)"
1000 INPUT VA$
1010 IF VA$ = "N" THEN GOTO 1260
1020 PRINT D$"OPEN":T$
1030 PRINT D$"WRITE":T$
1040 PRINT EX
1050 FOR I = 1 TO EX
1060 PRINT M(I)
1070 PRINT L(I)
1080 NEXT I: PRINT D$"CLOSE":T$

```

```

0010 E0 = 0
0020 IF E0 = 0 THEN EX
0030 E1 = E0 - (E0 * DI / 100):CS = E1 - (E0 * DI / 100)
0040 E2 = E1
0050 RETURN
0060 C1 = C1 - (C1 * DI / 100):CS = C1 - (C1 * DI / 100)
0070 IN = (CS - C1) / VI
0080 C1 = C1
0090 GOSUB 70
0100 GOSUB 2000
0110 E1 = E0
0120 IF E1 > E THEN GOTO 0080
0130 E = E1:CM = C1
0140 C1 = C1 + IN
0150 IF C1 < CS THEN GOTO 0080
0160 C1 = CM
0170 C1 = C2 - (C2 * DI / 100):CS = C2 + (C2 * DI / 100)
0180 IN = (CS - C1) / VI
0190 C2 = C1
0200 CM = C2
0210 GOSUB 70
0220 GOSUB 2000
0230 IF EC > E THEN GOTO 3180
0240 E = EC:CN = C2
0250 C2 = C2 + IN
0260 IF C2 < CS THEN GOTO 3140
0270 C2 = CN
0280 C1 = C3 - (C3 * DI / 100):CS = C3 + (C3 * DI / 100)
0290 IF C1 < CS THEN GOTO 3220
0300 CP = C1:C1 = CS:CS = CP
0310 IN = (CS - C1) / VI
0320 C3 = C1
0330 GOSUB 70
0340 GOSUB 2000
0350 IF EC > E THEN GOTO 3280
0360 E = EC:CO = C3
0370 C3 = C3 + IN
0380 IF C3 < CS THEN GOTO 3240
0390 C3 = CO
0400 U = 1
0410 GOTO 70
0420 IN = 1E - 2 * C1
0430 IO = IN
0440 GOSUB 70: GOSUB 2000
0450 E0 = E0
0460 PRINT "E0=";E0
0470 C1 = C1 + IN
0480 GOSUB 70: GOSUB 2000
0490 PRINT "EC=";E0: PRINT "C1=";C1
0500 IF E0 > E0 THEN GOTO 0560
0510 CP = C1:EP = E0
0520 C1 = C1 + IN:E0 = E0
0530 GOTO 0520
0540 IN = IN / 10
0550 IF IN < (1E - 3 * IN) THEN GOTO 0580
0560 C1 = CP:EP = EP: GOTO 0520
0570 GOSUB 70: GOSUB 2000
0580 PRINT "C1=";C1: PRINT "EC=";E0
0590 IF EC > E0 THEN GOTO 0610
0600 C1 = C1 - IN:E0 = E0
0610 GOTO 0570
0620 IN = IN / 10
0630 IF (ABS(IN) > ABS(1E - 4 * 10)) THEN GOTO 0620
0640 STOP

```


END
FILMED

5-86

DTIC